Article

Polymer-Metal Bilayer with Alkoxy Groups for Antibacterial Improvement

Hazem Idriss , Anna Kutová , Silvie Rimpelová , Roman Elashnikov , Zdeňka Kolská , Oleksiy Lyutakov , Václav Švorčík , Nikola Slepičková Kasálková , Petr Slepička *

Posted Date: 2 February 2024

doi: 10.20944/preprints202402.0177.v1

Keywords: polymer layer; PEG coating; alkoxy amine; titanium; stainless steel; grafting; hydrophilicity; biomaterials; medical devices

Article

Polymer-Metal Bilayer with Alkoxy Groups for Antibacterial Improvement

Hazem Idriss [1], Anna Kutová [1], Silvie Rimpelová [2], Roman Elashnikov [1], Zdeňka Kolská [3], Oleksiy Lyutakov [1], Václav Švorčík [1], Nikola Slepičková Kasálková [1] and Petr Slepička [1,*]

[1] Department of Solid-State Engineering, University of Chemistry and Technology Prague, Technická 3, 166 28 Prague, The Czech Republic
[2] Department of Biochemistry and Microbiology, University of Chemistry and Technology Prague, Technická 3, 166 28 Prague, The Czech Republic
[3] Faculty of Science, J. E. Purkyně University, 400 96 Usti nad Labem, The Czech Republic
* Correspondence: petr.slepicka@vscht.cz

Abstract: Many bio-applicable materials, medical devices, and prosthetics combine both polymer and metal components to benefit from their complementary properties. This goal is normally achieved by their mechanical bonding or casting only. Here, we report an alternative easy method for the chemical grafting of a polymer on the surfaces of a metal or metal alloys using alkoxy amine salt as a coupling agent. The surface morphology of the created composites was studied by various microscopy methods, and their surface area and porosity were determined by adsorption/desorption nitrogen isotherms. The surface chemical composition was also examined by various spectroscopy techniques and electrokinetic analysis. Elements distribution on the surface was determined and successful bonding of the metal/alloys on one side with the polymer on the other one was confirmed by alkoxy amine. The composites show significantly increased hydrophilicity, reliable chemical stability of the bonding even interaction with solvent for 30 cycles, and up to 95% less bacterial adhesion for the modified samples in comparison to pristine samples, i.e. the characteristics promising for their application in biomedical field, such as for implants, prosthetics etc. All this using universal, two-step procedures with minimal use of energy, and the possibility of producing it on a mass scale.

Keywords: polymer layer; PEG coating; alkoxy amine; titanium; stainless steel; diazotization; grafting; bacterial adhesion; medical devices

1. Introduction

Metals and metal alloys have been used in medicine for at least 5,000 years [1], and they have been irreplaceable for many years for their excellent mechanical properties, biocompatibility (in the case of noble metals such as gold) or bioactivity (e.g., the possibility to achieve osseointegration in the case of titanium alloys). However, the main problems with metal prosthesis were their bacterial attachment and colonization [2]. A bacteria-contaminated implants can cause, for example, acute cellular rejection [3]. As an alternative, in the second half of the 20th century, polymers were introduced into medicine and pharmacy. They brought along revolutionary solutions into the treatment of various disorders and diseases and helped in prosthetics [4,5], drug delivery [6,7] and wound healing [8].

Today, new polymers are continually being produced with better characteristics: outstanding and tissue-like mechanical properties [9,10] and excellent biocompatibility [11,12]. Their high plasticity (shaping as demanded) arises from the preparation methods, such as heat-driven polymerization [13] or usage of three-dimensional printers [14], by which the monomer is put into the meld of a desired shape before its polymerization.

Composites consisting of metallic and polymeric parts with significantly enhanced properties such as a perfect balance between flexibility and high toughness of the material [15] open new applications e.g., in a trans-tissue (bone and ligaments) region [16,17]. Conventionally, the composites are created using "mechanical" methods, consisting in smelting and casting, or polymer

 doi:10.20944/preprints202402.0177.v1

interlocking during polymerization. Such operations are typically performed under elevated temperatures or via exothermic reactions that are highly power-consuming, expensive, and unstable in certain cases. Also, there is always a possibility of generating internal or thermal stresses in the metals or unintended change in their original bio characteristics [18]. Hence, new methods of preparing such composites are still being sought.

One of them may consist of the covalent bond between these two materials, metal, and polymer. Many previous works showed that functional groups of some compounds have a high potential to achieve bonding between materials of quite several types [19]. The reduction of these functional groups through a variety of processes (e.g., spontaneous, or electrochemical diazotization) will create radicals, which can be utilized for covalent binding the rest of the compound onto the surfaces of almost any solid material [20–23].

Several studies on the chemical bonding of metals and polymers have been published up to now. Alageel *et al.* [24] presented the method for chemical binding of Ti to poly (methyl methacrylate), using aryldiazonium salt (*p*-phenylenediamine) as a coupling agent. This procedure leads to excellent enhancement of the mechanical properties of this composite compared to the reference samples. Related results were obtained via different pathway on alloy/polymer composite prepared by grafting the surface of polyamide 6 polymer with 4-nitrobenezenediazonium (NBD) salt using L-ascorbic acid (LAA). In this way an intermediary organic layer was created, leading to an enhancement of the mechanical properties of the resulting composite and an increase in its hydrophilicity [25]. Zheng *et al.* [26] described a successful bioinspired bridging between $Li_7La_3Zr_2O_{12}$ alloy nanofibers with poly (ethylene oxide) by using an azole-containing compound (Dynasylan Imeo). Although this method showed significant improvements in the characteristics of the resulting materials (mainly in tensile strength), this approach has limitations due to its dependence on the chemistry of the alloy of choice, which can decrease the universality and versatility of this method and prevent it from being applied over a long line of other alloys or metals. However, the chemical stability of the bonding needs is worthy of further study since, the "unbinding" can happen easily in environments common in biomaterial application.

In this work we present a low-cost and facile chemical approach for bonding metals/alloys with polymers via an alkoxy-functional group (R-O-R') as an intermediary agent. The method leads to the composite material with increased surface hydrophilicity, chemically stable bonding and enhanced bacterial anti-adhesive properties. The obtained results demonstrated that the alkoxy group is a favourable candidate to achieve coupling of metals/alloys with polymers and utilization of the advantageous properties of both. Prepared composites could find applications in new previously unexplored, biomedicine fields. With the main advantage of this method being the ability to apply it on theoretically any metal/alloy and polymers, because it does not depend on their chemistry, but on the properties of the alkoxy amine.

2. Materials and Methods

To achieve the maximum usability of the resulting composite material in various applications a relevant metal/alloy and polymer had to be chosen. Considering the possibility to integrate the properties of both, we selected foils of titanium (99.6 %, 0.5 mm, Goodfellow, UK) as the metal, and foils of stainless steel (SS) AISI 316 (0.5 mm, Goodfellow, UK) as metal alloy. Both types of foils were cut into 10×10 mm^2 samples and cleaned by ultrasound in acetone and deionized water for 15 min each. These samples were split into two groups: (i) pristine samples to study the characterization and functionality before grafting and modification, and (ii) samples intended for grafting and modification.

As an additive polymer layer the polyethylene glycol (PEG) was selected for its variety of applications and facile manipulation. We used PEG (Goodfellow, UK) of different molecular weights, specifically liquid (Mn of 400) and crystals (Mn of 6,000), that were dissolved in methanol at a concentration of 1.3 mM and stirred in ultrasound until the solution was fully transparent and homogenous.

 doi:10.20944/preprints202402.0177.v1

2.1. Salt preparation and reduction

For the grafting process, alkoxy amine was prepared according to the method described earlier [27]. The salt reduction process started with dissolving 0.07 g of *p*-toluene sulfonic acid (P-TSOH) in 1 mL of acetic acid (CH_3COOH) at room temperature (RT). After complete dissolving, 0.03 mL of *tert*-butyl nitrite was added gradually to the mixture and stirred with a magnetic stirrer, until a homogenous solution was formed. After that, $2.5 \cdot 10^{-3}$ g of the alkoxy amine was added to the solution and stirred for 40 min. Finally, diethyl ether was used and added to the solution with a ratio of 1:1 and centrifuged at a speed of 7,500 rpm for 30 min until full decantation of the salt. Then the salt was washed and centrifuged one more time with diethyl ether. The remaining salt is reduced alkoxy amine diethyl (1-((1-(4- amino phenyl) ethoxy) (tert-butyl) amino)-2,2-dimethyl propyl) phosphonate.

2.2. Chemical grafting

An aqueous solution of the reduced alkoxy amine with a concentration of 5.7 M was prepared, into which the pristine samples of Ti and stainless steel were immersed for 30 min. at room temperature 25 °C. Subsequently, the samples were washed with deionized water (3×) and then with 98 % (*v*/*v*) methanol (3×).

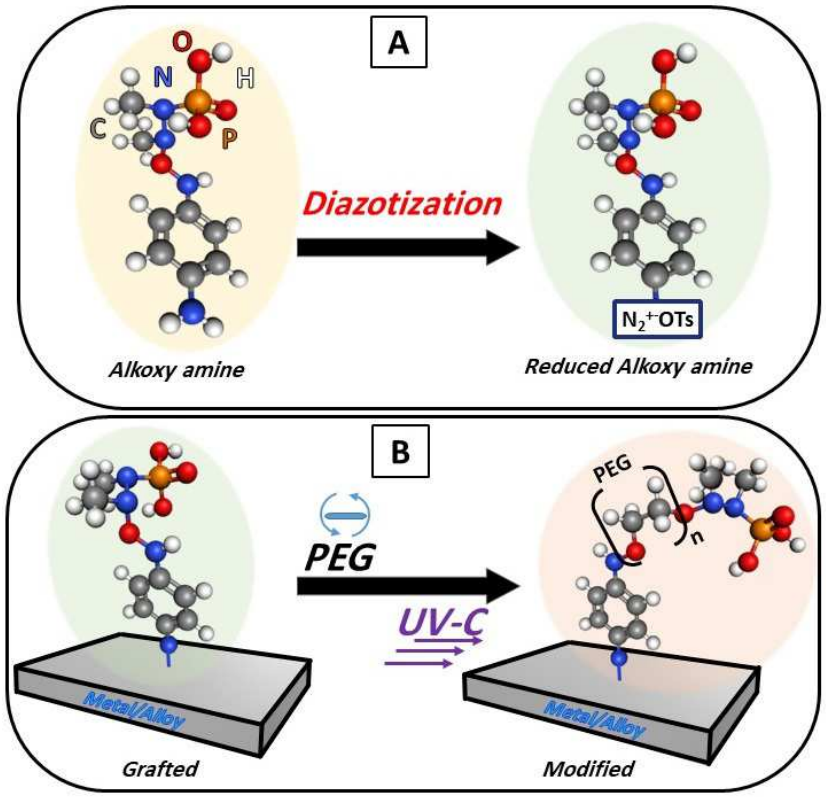

Figure 1. Schematic representation of salt diazotization, formation alkoxy amine groups on the surfaces (A) followed by surface grafting and modification of the surface with PEG (B).

2.3. Surface modification

The polymer solutions were deposited on the surface of the grafted samples by spin coater (1,000 rpm, 1 min) to produce a homogeneous polymer layer of unified thickness. To initiate the coupling, a source of UV-C light (280 nm, with intensity 2000 mW/cm^2) was used for 1 h at the distance of 2 cm from the samples. The chemical grafting and surface modification steps are demonstrated in Figure 1.

 doi:10.20944/preprints202402.0177.v1

2.4. Methods of characterization

To confirm the chemical bonding between the surface of metal/alloys and the organic layer on one side and then, between the organic layer with the polymer on the second side, Raman spectroscopy was measured on portable ProRaman-L spectrometer (Laser power 15 mW) Raman spectrometer with 785 nm excitation wavelength. Spectra were measured 30 times, each of them with 3 s accumulation time to detect the vibrational modes of molecules involved. Further, the technique of surface-enhanced Raman spectroscopy (SERS) was used to generate a peak distribution map of the activated and reduced salt on the surface of the grafted samples. The usage of the SERS technique was chosen for the mapping due to the high accuracy of detection (single molecule level) to give precise distribution map of the activated, reduced, and grafted alkoxy amine, which the usage of the standard Raman is not able to constrict, and to stack the spectra accurately at this stage of the modification process.

Changes in the surface roughness (R_a) of pristine samples (SS or Ti) before and after the grafting and the deposition of the polymer were measured by a confocal laser scanning microscope (CLSM; Olympus OLS 3100) using magnification lens (x50) without optical zoom, the roughness was calculated using the automatic calibration and it was collected from 10 different positions and then the average was calculated to acquire accurate roughness on a micron scale.

The electrokinetic potential of all samples was determined by SurPASS instrument (Anton Paar, Austria) in a cell with an adjustable gap at RT and pH of 6.7. The experimental error of the measurement was ± 5 %. For the determination of the zeta potential, the streaming current method and the Helmholtz-Smoluchowski equation were used. Specific surface area and pore volume were determined from nitrogen adsorption/desorption isotherms with a NOVA3200 (Quantachrome Instruments) using NovaWin software. The samples were degassed for 24 h at 60 °C. Brunauer-Emmett−Teller (BET) analysis was applied to determine the total surface area and Barrett−Joyner−Halenda (BJH) model for pores volume.

The spatial distributions and the concentrations of the surface elements for both stainless steel and titanium (pristine and modified) were characterized by Scanning Electron Microscopy (SEM) with embedded Energy Dispersive X-ray Spectroscopy (EDX) (Tescan Lyra 3 GMU). The X-ray photoelectron spectroscopy (XPS) was performed using an Omicron Nanotechnology ESCAProbeP spectrometer fitted with monochromated Al K Alpha X-ray source working at 1486.6 eV, to study the composition and these results were also used to determine the thickness of the layer (organic layer + polymer) as was demonstrated before [28]. For this purpose the well known equation $I/I_0=exp(-d/\lambda \sin\theta)$ was used, where d is the layer thickness, λ is the free path of the photoelectron in the organic layer, angle θ with respect to the plain surface was 90° and I/I_0 is the ratio of detected intensities of the elements Fe/Ti before and after the modification.

Sample functionalities were extensively studied, starting with their surface wettability, which is supposed to radically shifted after the polymer application and by the electrokinetic analyses. The wettability tests consist of measuring the static and the dynamic water contact angle (WCA) by goniometer Krüss (DSA 100). For static angle, deionized water droplets with a volume of 2 μL were dropped on 10 different positions on the surface of both pristine and modified samples. The dynamic CA measurements were performed by deposition of the water drop on the sample surface, followed by increasing and subsequent decreasing of the water drop volume variating between values of 2-10 μL with a speed increase/decrease by 0.03 mL·min^{-1}, with simultaneous measurements of the contact angle.

The wettability tests were also used to evaluate the chemical stability of the bond. Two sets of samples were prepared (i) the first one consisting of modified samples of titanium or stainless steel as aforementioned and (ii) the second one of titanium or stainless steel with a deposited layer of the polymer modified under the same conditions but without the grafting step on the surface (i.e. metal/alloy with deposited PEG only). Both sample sets were soaked in deionized water for 30 min, air-dried, and measured by the goniometer one more time. The changes in WCA were measured at various positions and repeatedly for 30 times. The establishment of chemical bonding will protect the polymer from being dissolved in water and will keep the WCA stable at hydrophilic values. In the

 doi:10.20944/preprints202402.0177.v1

case of missing chemical bonding, the polymer dissolves and the goniometer reading should indicate significant changes in WCA.

Further, we have studied the bacterial anti-adhesive activity of the prepared materials. For this purpose, two bacterial strains were chosen: i) *Escherichia coli* (*E. coli,* DBM 3138) as a model of *Gram-negative* bacteria and *Staphylococcus epidermidis* (*S. epidermidis*, DBM 2124) as a model of *Gram-positive* bacteria. Both bacterial strains were from the microorganism collection of the Department of Biochemistry and Microbiology at the UCT Prague (Czech Republic). To assess the bacterial anti-adhesive potential of the prepared materials, we used the drop plate method similarly as reported in [29,30]. First, Luria-Bertani (LB) liquid medium was inoculated with one colony-forming unit (CFU) of either *E. coli* or *S. epidermidis* [31,32] and cultivated in an orbital shaker at 120 rpm at 37 °C for 18 h. Then, the inocula were diluted in phosphate-buffered saline (PBS, sterile) of pH = 7.4 to achieve three concentrations, i.e., 8×10^8, 4×10^7, and 1×10^4 of *E. coli* and *S. epidermidis* per mL. The evaluated samples were immersed into the bacterial suspensions and evaluated in triplicates. Then, the samples were incubated at room temperature for 1, 4, and 24 h while gently shaking. After these time points, 25-μL aliquots in five technical replicates were taken from each sample (after gentle mixing), loaded onto pre-dried LB agar plates, and incubated at 37 °C for 24 h. As a control, bacteria cultivated only in PBS, without a material sample addition, were used as well as bacterial suspensions cultivated with pristine Ti and pristine SS. After the 24-h incubation, the numbers of CFU of each bacterial strain were counted using Image J software.

In addition, to examine the bacteria incubated with the evaluated materials in greater detail, an SEM analysis of the samples was performed. After 24 h of incubation, the samples were gently washed with 1 mL of PBS and then fixed using the mixture of 2 % formaldehyde with 2.5 % glutaraldehyde in PBS for 4 h, at RT (ca 23 °C). After that, the samples were gently washed with PBS two times and then dehydrated similarly as described in refs. [33,34]. Briefly, the samples were incubated with ethanol solutions in water for 10 min in the following order: ethanol: water (*v*/*v*): 50, 60, 70, 80, 90, and 98 %. After that, hexamethyl disiloxane (Sigma Aldrich, USA) was added for 10 min twice, and then got removed and then the samples were dried at 37 °C for 16 h, which was followed by sputtering of a 5-nm platinum layer, and then studied by (SEM) at 10 different positions.

3. Results and Discussion

The process of chemical coupling of titanium (Ti) or stainless steel (SS) with PEG can be described as a two-step procedure; (i) the reduction of the salt as demonstrated, left free radicals which allows the salt to be grafted on the surfaces of any solid material (here Ti, and SS) and (ii) deposition of the PEG and then using UV-C led to the homolysis of the N-O bond which formed radicals on the other end of the reduced salt allowing the bonding for both PEG 400 and PEG 6,000. However, the WCA measurements of PEG 6000 showed more hydrophilic character, therefore the following measurements are mainly focused on PEG 6000.

The successful grafting of the salt was confirmed by Raman spectroscopy with new peaks appearing in the gathered spectra. These new peaks are found at Raman shift 450-500 cm^{-1} and 1,400 and 1,600 cm^{-1} for the aromatic ring, 550-600 cm^{-1}, 700 cm^{-1}, and 1300 cm^{-1} for Isopropyl (i-pr), 800-900 cm^{-1} and 1,300 cm^{-1} for N-O, 1,100 cm^{-1} and 1,320-1,350 cm^{-1} for P=O, and finally at 1,200 cm^{-1} for C-N [35]. Also the successful modification with PEG 6,000 can be confirmed by the changes in certain peaks , related to the interaction of PEG 6,000 with the salt (see Figure 2 A, B). These are related to the break of the N-O bond and disappearance of the peak at 1,300 cm^{-1} and forming a new C-O bond between 1,350 and 1,400 cm^{-1}. Moreover, the homogenous distribution of the activated reduced salt on the surface of the stainless steel and the titanium was confirmed by SERS (see Figure 2C, D).

Preprints.org (www.preprints.org) | NOT PEER-REVIEWED | Posted: 2 February 2024 doi:10.20944/preprints202402.0177.v1

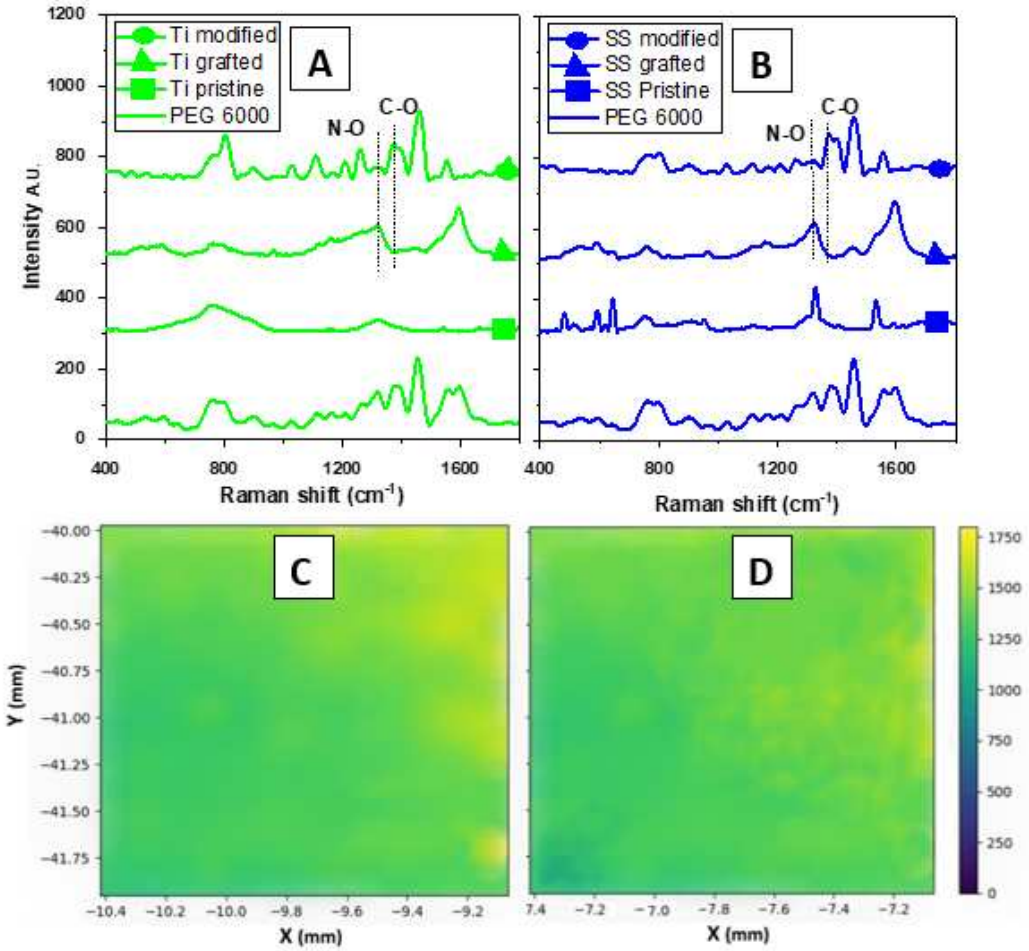

Figure 2. The Raman spectra of pristine, grafted, modified Ti (A) and SS (B) samples, and Raman mapping of the significant peaks of alkoxyamine on the surface of the samples determined by the SERS technique for Ti (C) and SS (D).

The chemical composition of the samples before and after the modification were studied by EDX and XPS techniques. Results are presented in Table 1, where corresponding results of the concentrations of substrate elements (Fe, Cr, Ti, etc.) are shown. Both methods confirmed a dramatic increase in the concentrations of the alkoxy amine groups and the elements of the PEG 6,000 polymer such as C, O, and N on the surfaces after the modification for both of the substrates, with the biggest portion of the increase being for C (between 4-8%), O (4-6%), and N (1-2%) respectively, which correspond with the ratios of these atoms within the formula of PEG. It is also possible to notice the decrease of the elements forming the substrates only after the modification as the penetration of the analysis will be reduced because of the organic + polymer extra layer. As also can be seen, the percentage of elements forming PEG 6,000 is higher for the XPS than for EDX, due to the depth of analysis achievable by both individual techniques.

To calculate the thickness of the layer (d), we first calculated the value of λ which was deduced from the empirical formula derived by Seah and Dench: $\lambda_k = A_n/E^2_K + B_n/ E^{1/2}_K$· where E_k is the kinetic energy of photoelectrons.

After the calculations, it was found that the thickness of the organic/ polymer bonded with Ti/ SS layer is found to be d ≈2.8 nm and d≈2.7 nm, respectively.

 doi:10.20944/preprints202402.0177.v1

Table 1. Element surface concentration determined by XPS and EDX for both titanium and stainless steel for pristine and modified samples.

Element	***Analytic methods***			
	XPS *(at. %)*		**EDX** *(at. %)*	
	Titanium			
	Pristine	***Modified***	***Pristine***	***Modified***
C	35	39	4	11
O	40	44	3	6
N	0	1	0	1
Ti	25	16	93	82
	Stainless steel			
	Pristine	***Modified***	***Pristine***	***Modified***
C	48	56	8	11
O	28	34	1	2
N	0	2	0	1
Fe	17	5	63	61
Cr	4	2	17	15
Ni	3	1	11	10

The data gathered from the CLSM showed that the surface roughness R_a of both pristine and modified samples for SS stayed almost unchanged at R_a of ca. 1.4 μm to 1.3 μm after the modification. For Ti samples, however, the surface roughness slightly decreased after the modification from R_a of ca. 1.8 to 1.2 μm. However, no significant changes in the surface morphology were observed by the SEM technique, with minor changes can be noticed on the original topography of the Ti (see Figure 3 A pristine Ti, and B pristine SS, C modified Ti, and D modified SS).

The changes in the surface roughness of the samples before and after the modification were proven also from the surface area and porosity values determined by adsorption/desorption nitrogen isotherms presented in Table 1. The surface area and porosity increased after the modification of both stainless steel and Ti with changes more apparent for Ti samples.

Changes in surface chemistry and polarity were confirmed also by electrokinetic analysis. The values of zeta potential are presented in Table 2 (the last row). These results are quite interesting, after the modification, when the zeta potentials changed differently for both substrates, SS and Ti. For SS, the zeta potential changed to lower negative values, from -51.3 ± 2.8 mV for pristine SS surface to -39.0 ± 2.3 mV for modified one, which change indicates some positively charged groups on the surface (presence of amino- groups) [36]. The Ti surface, however, shows after the modification more negative values of zeta potential -52.1 ± 5.6 mV in comparison with -45.7 ± 1.4 mV for the pristine Ti surface. The change can be affirmed to more negatively charged oxygen groups on the modified surface of Ti. The diazotization process has the potential to introduce negatively charged groups onto the surface of titanium (Ti). During diazotization, a diazonium salt is typically formed, and the resulting diazonium group can be covalently attached to the Ti surface. The presence of nitrogen in the diazonium group, especially in the form of a negatively charged nitrosonium ion (NO^+), can contribute to the overall charge of the modified surface. As, was reported previously, some compounds bonds to the different surfaces differently with a preferential orientation of some functional groups depending on the polar/unipolar behaviour or different roughness of substrates surfaces [36]. These results can be confirmed by XPS measurement (Table 1). Here is clear the amount of N groups is 0 at unmodified samples (both Ti and SS), while after modification, the amount of N groups is visible and it is slightly higher at modified SS, therefore that means the higher amount of

 doi:10.20944/preprints202402.0177.v1

amino- groups on the surface at SS and this resulted in less negative zeta potential at modified SS in comparison with modified Ti. We can also see the amount of oxygen groups (O amount), which has impact on the negative surface charge. As it is clear, the higher amount of O groups was determined in both cases at Ti samples. Therefore, the zeta potential is much negative for Ti samples (pristine and modified ones) in comparison with SS samples.

Table 2. Surface area, pore volume and electrokinetic potential (zeta potential ζ) of individual samples for stainless steel and titanium samples in pristine and modified forms.

	Titanium		**Stainless steel**	
	Pristine	***Modified***	***Pristine***	***Modified***
Surface area ($m^2.g^{-1}$)	9.7 ± 2.7	14.3 ± 0.8	8.3 ± 0.1	10.9 ± 2.1
Pore volume ($cm^3.g^{-1}$)	11.0 ± 1.0	16.0 ± 0.4	9.0 ± 1.0	11.0 ± 2.0
Zeta potential (mV)	-45.7 ± 1.4	-52.1 ± 5.6	-51.3 ± 2.8	-39.0 ± 2.3

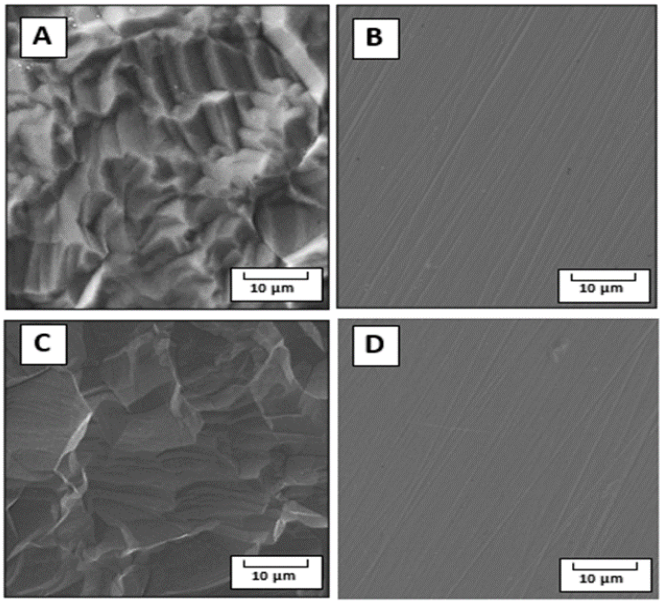

Figure 3. The surface morphology of the samples as observed by SEM for pristine Ti (A) and pristine SS (B), Ti modified (C) and SS modified (D).

The modification of the samples leads to an increase in the wettability of the surfaces of the composites, manifested by lower contact angle, WCA. This was confirmed using both dynamic and static WCA goniometry. As can be seen from Figure 4A, the static WCA significantly decreased after the material modifications, the decrease being especially large for PEG 6,000, consisting of longer chains in comparison with PEG 400. Also, the dynamic WCA results corresponds with those obtained by static WCA; the hydrophilic surface was kept at similar values whether the droplet volume was advancing or receding, in contrast to the case of the more hydrophobic pristine samples. These exhibits bigger differences, which is one of the common properties of hydrophobic surfaces, see Figure 4B. These results are the same for all substrates and they correspond well with those from zeta potential tests.

The results of the chemical stability tests show, higher performance of the modified samples after immersing in water. As was anticipated, the immersion leads to the dissolving of the PEG

 doi:10.20944/preprints202402.0177.v1

deposited layer, which was not pre-grafted, leading to instant "collapse" of the composite hydrophilic character. In the case the modified samples with the help of the grafted salt the PEG 6,000 chains stay attached to the surface (see Figure 4C). These findings are specifically important in showing the durability of the modified composites, which can be able to survive the next step which is the tests of their bacterial anti-adhesive properties.

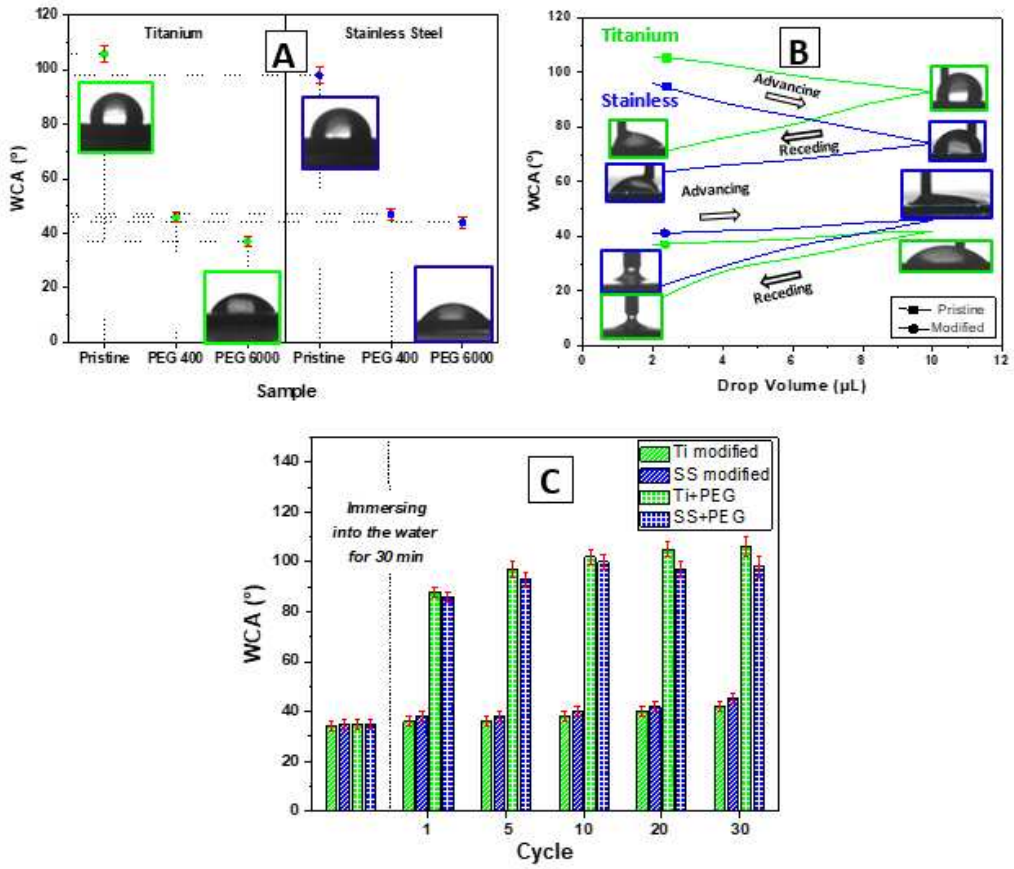

Figure 4. Static water contact angle (A); dynamic water contact angle (WCA) determined for individual samples by goniometry (B); chemical stability measured by changes in WCA after immersion of the samples into the water and measuring of WCA (C).

The bacterial anti-adhesive properties of the prepared materials were determined by CFU counting of two bacterial strains of *S. epidermidis* and *E. coli*, which were in contact with the evaluated samples for 4 h. For this purpose, three concentrations of bacterial inocula were chosen, i.e., 8×10^8, 4×10^7, and 1×10^4 per mL. As for *E. coli*, at the two higher concentrations, 4 h contact with the prepared materials did not result in a decrease in number of grown bacteria. However, for *S. epidermidis* at 8×10^8 concentration, there was ca 20 % decrease in the bacteria grown when incubated with modified Ti or SS samples, which was further pronounced to a ca 60 % decrease at lower, 4×10^7 per mL, concentration of bacteria for modified SS samples (data not shown) in comparison to untreated control as well as pristine samples. Notably, at the lowest concentration of bacteria, i.e., 1×10^4 per mL, the modified Ti or SS impacted the number of both bacterial strains *E. coli* and *S. epidermidis*, see Figure 5A. At these conditions, there was ca 30 % decrease in the *E. coli* CFU number after 4 h incubation with pristine and modified SS and pristine Ti. Even more pronounced effect on lower adhesion of bacteria had modified Ti, the 4 h contact of which with the bacteria resulted in reduction of *E. coli* CFU number by ca 70 %. Interestingly, for *S. epidermidis* at the concentration of bacteria 1×10^4 per mL, the inhibition efficiency of modified Ti and SS samples after 4 h incubation differed from that for *E. coli*. Here, the most efficient in bacterial growth inhibition was modified SS, the presence of which resulted in a decrease of *S. epidermidis* CFU number by ca 95 %, while modified Ti by ca 50 %.

 doi:10.20944/preprints202402.0177.v1

In contrast to the results gained for *E. coli*, no effect on the CFU number of *S. epidermidis* was detected for pristine Ti and SS. These results were further confirmed by SEM images of the bacteria on all types of samples, see Figure 5B, C. Moreover, the data from SEM analysis document that only a negligible number of bacteria of both strains adhered on modified Ti and SS samples when compared to heavily colonized pristine samples.

The differences between the observed adhesive behaviour can be understood by the original surface characteristics of the substrate (namely, surface area, porosity, and roughness) which are different between the SS and Ti as shown before, and by the original biocompatibility. Also from the way, each bacterial strain adheres to the surface (surface binding with different proteins in the case of *E.coli* and *S. epidermidis*) [37,38]. However, all samples showed less adhesion of bacteria after the bonding, which means that the surface would become more bacteria resistant, which might protect medical devices from causing infections, or even rejection of prosthetics.

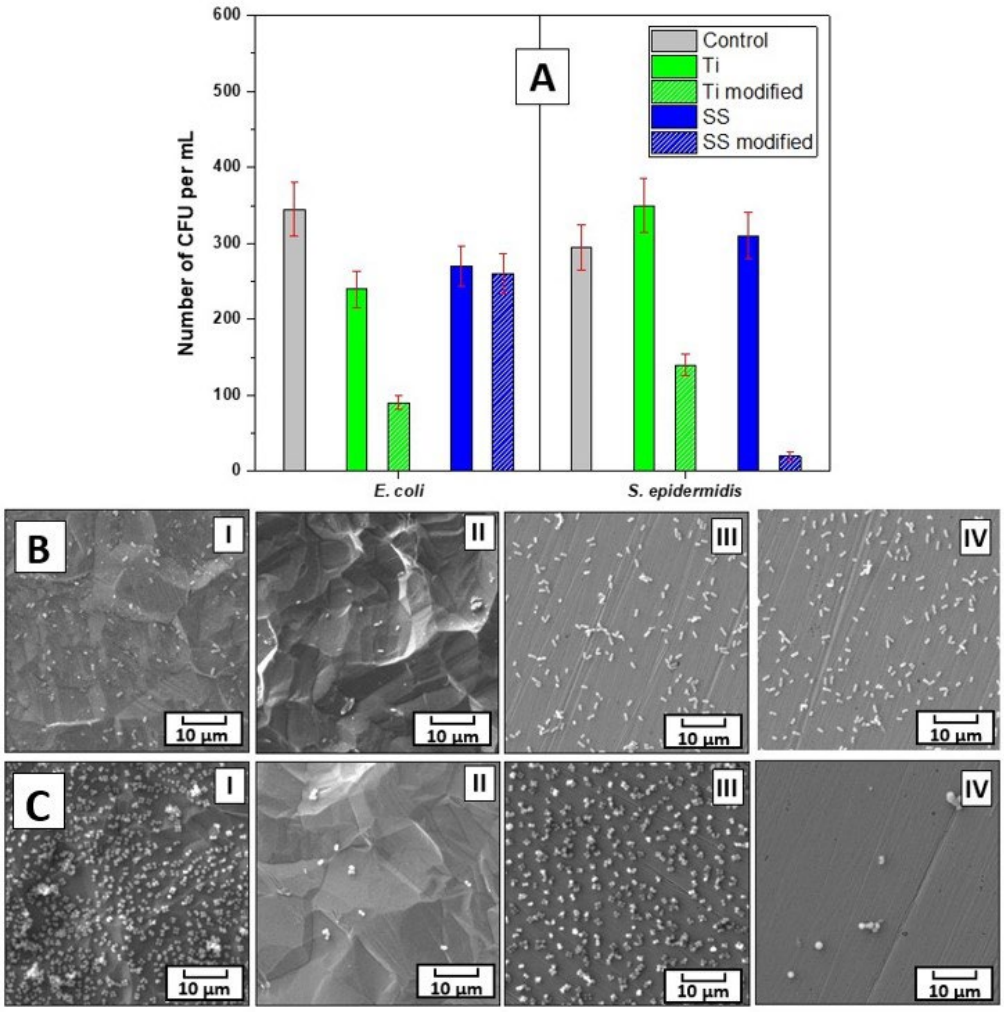

Figure 5. The number of colony-forming units (CFU) of S. epidermidis and E. coli incubated for 4 h with the pristine and modified Ti and SS samples (A). SEM images of S. epidermidis (B) E. coli (C) on pristine and modified Ti (I and II, respectively) and stainless steel pristine and modified (III and IV respectively).

5. Conclusions

In this study, we demonstrated a universal, alternative approach to the conventional methods to "bond" Ti or Stainless-steel surface with PEG via grafting of alkoxyamine. The successful chemical bonding was demonstrated by Raman measurements and changes in the element concentrations, confirmed by EDX and XPS measurements. The successful modification result in the significant changes of surface properties of the materials which were clearly shown by wettability and surface

area and zeta potential measurements. This chemical bonding technique makes possible to fabricate composites with reliable stability in water solutions after 30 cycles, and several useful functionalities. Therefore this bonding technique deserves closer research and the applications not only to biomaterials but also in another fields. Modified Ti has shown good bacterial anti-adhesive properties against both *E. coli* and *S. epidermidis*, while modified SS only against the *S. epidermidis*. Therefore, both modified Ti and SS have high potential as bacterial anti-adhesive surfaces.

Author Contributions: Conceptualization, H.I., A.K. and R.E.; methodology, Z.K. and N.S.K.; validation, V.S. and O.L. ; formal analysis Z.K.; investigation, H.I., S.R. , R.E. and O.L.; data curation, P.S and N.S.K.; writing—original draft preparation, H.I.; writing—review and editing, P.S. and S.R.; supervision, O.L..; funding acquisition, V.S and N.S.K. All authors have read and agreed to the published version of the manuscript.

Funding: This work was supported by the GACR under the project No. 22-25734S, this work was also supported by the Project ExRegMed, No CZ.02.01.01/00/22_008/0004562, of the Ministry of Education, Youth and Sports, which is co-funded by the European Union.

Institutional Review Board Statement: Not applicable.

Conflicts of Interest: The authors declare no conflicts of interest.

References

1. Medici, S.; Peana, M.; Nurchi, V.M.; Lachowicz, J.I.; Crisponi, G.; Zoroddu, M.A. Noble Metals in Medicine: Latest Advances. Coord. Chem. Rev. 2015, 284, 329–350. doi:10.1016/j.ccr.2014.08.002.
2. Ramezani, M.; Monroe, MBB. Bacterial protease-responsive shape memory polymers for infection surveillance and biofilm inhibition in chronic wounds. J. Biomed. Mater. Res. A. 2023, 7, 921-937. doi: 10.1002/jbm.a.37527
3. Banerjee, D.; Nayakawde, NB.; Antony, D.; Deshmukh, M.; Ghosh, S.; Sihlbom, C.; Berger, E.; Ul Haq, U.; Olausson, M. Characterization of Decellularized Implants for Extracellular Matrix Integrity and Immune Response Elicitation. Tissue Eng. Part A. 2022, 28, 621-639. doi: 10.1089/ten.tea.2021.0146
4. Powell, S.K.; Cruz, R.L.J.; Ross, M.T.; Woodruff, M.A. Past, Present, and Future of Soft-Tissue Prosthetics: Advanced Polymers and Advanced Manufacturing. Adv. Mater. 2020, 32, 2001122. doi:10.1002/adma.202001122.
5. Williams, J.O.D.; Solan, G.A.; Xu, J.; Allen, J.; Harris, R.C.; Timmermann, V.M. Investigating Branched Polyethylene Sensors for Applications in Prosthetics. Macromol. Chem. Phys. 2021, 222, 2100206. doi:10.1002/macp.202100206.
6. Hogan, K.J.; Mikos, A.G. Biodegradable Thermoresponsive Polymers: Applications in Drug Delivery and Tissue Engineering. Polymer 2020, 211. doi:10.1016/j.polymer.2020.123063.
7. Liu, L.; Tang, H.; Wang, Y. Polymeric biomaterials: Advanced drug delivery systems in osteoarthritis treatment, Heliyon 2023, 9, e21544. doi.org/10.1016/j.heliyon.2023.e21544.
8. Kutová, A.; Staňková, L.; Vejvodová, K.; Kvítek, O.; Vokatá, B.; Fajstavr, D.; Kolská, Z.; Brož, A.; Bačáková, L.; Švorčík, V. Influence of Drying Method and Argon Plasma Modification of Bacterial Nanocellulose on Keratinocyte Adhesion and Growth. Nanomaterials 2021, 11. doi:10.3390/nano11081916.
9. Sawadkar, P.; Mandakhbayar, N.; Patel, K.D.; Buitrago, J.O.; Kim, T.H.; Rajasekar, P.; Lali, F.; Kyriakidis, C.; Rahmani, B.; Mohanakrishnan, J.; et al. Three Dimensional Porous Scaffolds Derived from Collagen, Elastin and Fibrin Proteins Orchestrate Adipose Tissue Regeneration. J Tissue Eng 2021, 12, 204173142110192. doi:10.1177/20417314211019238.
10. Jiang, X.; Zhang, K.; Huang, Y.; Xu, B.; Xu, X.; Zhang, J.; Zhang, G. Conjugated Microporous Polymer with C≡C and C–F Bonds: Achieving Remarkable Stability and Super Anhydrous Proton Conductivity. ACS Appl. Mater. Interfaces. 2021, 13, 15536–15541. doi:10.1021/acsami.1c02355
11. Gao, S.; Tang, G.; Hua, D.; Xiong, R.; Han, J.; Jiang, S.; Zhang, Q.; Huang, C. Stimuli-Responsive Bio-Based Polymeric Systems and Their Applications. J. Mater. Chem. B 2019, 7, 709–729. doi:10.1039/C8TB02491J.
12. Chan, Doreen; Maikawa, Caitlin L.; d'Aquino, Andrea I.; Raghavan, Shyam S.; Troxell, Megan L.; Appel, Eric A. Polyacrylamide-based hydrogel coatings improve biocompatibility of implanted pump devices. J. Biomed. Mater. Res. A. 2023, 7, 910-920. doi: 10.1002/jbm.a.37521
13. Robert, C.; Mamalis, D.; Obande, W.; Koutsos, V.; Ó Brádaigh, C.M.; Ray, D. Interlayer Bonding between Thermoplastic Composites and Metals by IN-SITU Polymerization Technique. J Appl Polym Sci. 2021, 138, 51188. doi:10.1002/app.51188.

14. Idriss, H.; Elashnikov, R.; Rimpelová, S.; Vokatá, B.; Haušild, P.; Kolská, Z.; Lyukatov, O.; Švorčík, V. Printable Resin Modified by Grafted Silver Nanoparticles for Preparation of Antifouling Microstructures with Antibacterial Effect. Polymers. 2021, 13, 3838. doi:10.3390/polym13213838.
15. Xu, R.; Xie, Y.; Li, R.; Zhang, J.; Zhou, T. Direct Bonding of Polymer and Metal with an Ultrahigh Strength: Laser Treatment and Mechanical Interlocking. Adv. Eng. Mater. 2021, 23, 2001288. doi:10.1002/adem.202001288.
16. Kafkopoulos, G.; Padberg, C.; Duvigneau, J.; Vancso, G. Adhesion Engineering in Polymer–Metal Comolded Joints with Biomimetic Polydopamine, ACS Appl. Mater. Interfaces. 2021, 13, 19244-19253. doi: 10.1021/acsami.1c01070
17. Singh, G.; Santhanakrishnan, S. Fabrication and Characterization of Composite PMMA/HA Scaffold Using Freeze Casting Method. Adv. Perform. Mater. 2021, 37, 1–8. doi:10.1080/10667857.2021.1978640.
18. Lu, X.; Lin, X.; Chiumenti, M.; Cervera, M.; Hu, Y.; Ji, X.; Ma, L.; Huang, W. In Situ Measurements and Thermo-Mechanical Simulation of Ti–6Al–4V Laser Solid Forming Processes. Int. J. Mech. Sci. 2019, 153–154, 119–130. doi:10.1016/j.ijmecsci.2019.01.043.
19. Mahouche-Chergui, S.; Gam-Derouich, S.; Mangeney, C.; Chehimi, M.M. Aryl Diazonium Salts: A New Class of Coupling Agents for Bonding Polymers, Biomacromolecules and Nanoparticles to Surfaces. Chem. Soc. Rev. 2011, 40, 4143. doi:10.1039/c0cs00179a.
20. Idriss, H.; Guselnikova, O.; Postnikov, P.; Kolska, Z.; Haušild, P.; Čech, J.; Lyutakov, O.; Švorčík, V. Versatile and Scalable Icephobization of Airspace Composite by Surface Morphology and Chemistry Tuning. ACS Appl. Polym. Mater. 2020, 2, 977–986. doi:10.1021/acsapm.9b01185.
21. Kim, J.; Choi, J.-H.; Sung, M.; Yu, W.-R. Improved Adhesion of Metal–Polymer Sandwich Composites Using a Spontaneous Polymer Grafting Process. Funct. Compos. Struct. 2019, 1, 025004, doi:10.1088/2631-6331/ab267b.
22. Idriss, H.; Elashnikov, R.; Guselnikova,O.; Postnikov, P.; Kolska, Z.; Lyutakov, O.; Švorčík, V. Reversible wettability switching of piezo-responsive nanostructured polymer fibers by electric field, Chem. Pap. 2020, 75, 191–196, doi:10.1007/s11696-020-01290-3.
23. Ma, GL.; Candra, H.; Pang, LM.; Xiong, J.; Ding, YC.; Tran, HT.; Low, ZJ.; Ye, H.; Liu, M.; Zheng, J.; Fang, ML.; Cao, B.; Liang, ZX. Biosynthesis of Tasikamides via Pathway Coupling and Diazonium-Mediated Hydrazone Formation, J. Am. Chem. Soc. 2022,4, 1622-1633. doi: 10.1021/jacs.1c10369
24. Alageel O, Abdallah MN, Luo ZY, Del-Rio-Highsmith J, Cerruti M, Tamimi F. Bonding metals to poly (methyl methacrylate) using aryldiazonium salts. Dent Mater. 2015, 31,105-14. doi: 10.1016/j.dental.2014.11.002.
25. Martin, K.L.; Parvulescu, M.J.S.; Patel, T.A.; Mogilevsky, P.; Key, T.S.; Thompson, C.M.; Dickerson, M.B. Bioinspired Cross-Linking of Preceramic Polymers via Metal Ion Coordination Bonding. J. Eur. Ceram. Soc. 2021, 41, 6366–6376. doi:10.1016/j.jeurceramsoc.2021.05.046.
26. Zheng, X.; Wei, J.; Lin, W.; Ji, K.; Wang, C.; Chen, M. Bridging Li 7 La 3 Zr 2 O 12 Nanofibers with Poly(Ethylene Oxide) by Coordination Bonds to Enhance the Cycling Stability of All-Solid-State Lithium Metal Batteries. ACS Appl. Mater. Interfaces 2022, 14, 5346–5354. doi:10.1021/acsami.1c21131.
27. Audran, G.; Brémond, P.; Joly, J.-P.; Marque, S.R.A.; Yamasaki, T. C–ON Bond Homolysis in Alkoxyamines. Part 12: The Effect of the Para-Substituent in the 1-Phenylethyl Fragment. Org. Biomol. Chem. 2016, 14, 3574–3583. doi:10.1039/C6OB00384B.
28. Gehan, H.; Fillaud, L.; Chehimi, M.M.; Aubard, J.; Hohenau, A.; Felidj, N.; Mangeney, C. Thermo-Induced Electromagnetic Coupling in Gold/Polymer Hybrid Plasmonic Structures Probed by Surface-Enhanced Raman Scattering. ACS Nano 2010, 4, 6491–6500. doi:10.1021/nn101451q.
29. Hurtuková, K.; Fajstavrová, K.; Rimpelová, S.; Vokatá, B.; Fajstavr, D.; Kasálková, N.S.; Siegel, J.; Švorčík, V.; Slepička, P. Antibacterial Properties of a Honeycomb-like Pattern with Cellulose Acetate and Silver Nanoparticles. Mater. 2021, 14, 4051, doi:10.3390/ma14144051.
30. Slepička, P.; Rimpelová, S.; Slepičková Kasálková, N.; Fajstavr, D.; Sajdl, P.; Kolská, Z.; Švorčík, V. Antibacterial Properties of Plasma-Activated Perfluorinated Substrates with Silver Nanoclusters Deposition. Nanomater. 2021, 11, 182. doi:10.3390/nano11010182.
31. Aggarwal, D.; Kumar, V.; Sharma, S. Drug-loaded biomaterials for orthopedic applications: A review, J. Controlled Release 2022, 344, 113–133. doi.org/10.1016/j.jconrel.2022.02.029

32. Rodríguez-Sánchez, J.; Pacha-Olivenza, M. A.; González-Martín, M. L. Bactericidal effect of magnesium ions over planktonic and sessile *Staphylococcus epidermidis* and *Escherichia coli*, Mater. Chem. Phys. 2019, 221, 342-348, doi.org/10.1016/j.matchemphys.2018.09.050.
33. Slepička, P.; Michaljaničová, I.; Rimpelová, S.; Švorčík, V. Surface Roughness in Action – Cells in Opposition. Mater. Sci. Eng. C. 2017, 76, 818–826. doi:10.1016/j.msec.2017.03.061.
34. Slepička, P.; Peterková, L.; Rimpelová, S.; Pinkner, A.; Slepičková Kasálková, N.; Kolská, Z.; Ruml, T.; Švorčík, V. Plasma Activated Perfluoroethylenepropylene for Cytocompatibility Enhancement. Polym. Degrad. Stab. 2016, 130, 277–287. doi:10.1016/j.polymdegradstab.2016.06.017.
35. Socrates, G. Infrared and Raman Characteristic Group Frequencies: Tables and Charts; 3rd ed.; Wiley: Chichester; New York, 2001.
36. Kosmulski, M.; Maczka, E. Zeta potential in dispersions of titania nanoparticles in moderately polar solvents stabilized with anionic surfactants, J. Mol. Liquids 2022, 355, 118972, doi.org/10.1016/j.molliq.2022.118972.
37. Elfazazi, K.; Zahir, H.; Tankiouine, S.; Mayoussi, B.; Zanane, C.; Lekchiri, S.; Ellouali, M.; Mliji, EM.; Latrache, H.; Adhesion Behavior of Escherichia coli Strains on Glass: Role of Cell Surface Qualitative and Quantitative Hydrophobicity in Their Attachment Ability. Int J Microbiol. 2021 Oct 7;2021:5580274. doi: 10.1155/2021/5580274
38. Nuno, C.; Gerald, B.; Pier, b.; Manuel, V.; Rosário, O.; Joana, A. Quantitative analysis of adhesion and biofilm formation on hydrophilic and hydrophobic surfaces of clinical isolates of Staphylococcus epidermidis. Research in Microbiology. 2005, 156. https://doi.org/10.1016/j.resmic.2005.01.007